

1 **Supplementary Information**

2  
3 **Water Transport Confined in Graphene Oxide Channels through Rarefied Effect**

4  
5 Bo Chen, Haifeng Jiang\*, Xiang Liu and Xuejiao Hu\*

6 Key Laboratory of Hydraulic Machinery Transients (Wuhan University), Ministry of Education, School of Power  
7 and Mechanical Engineering, Wuhan University, Wuhan, Hubei 430072, China

8 \*Corresponding authors. E-mail addresses: hfjiang@whu.edu.cn (H. Jiang), xjhu@whu.edu.cn (X. Hu).

9  
10  
11 **Contents**

12

|   |    |
|---|----|
| 13 1. Different distributions of hydroxyl groups in oxidized region ..... | 2  |
| 14 2. Contact angle tests .....   | 2  |
| 15 3. Free energy analysis.....   | 3  |
| 16 4. References.....   | 12 |

17  
18

## 1 **1. Different distributions of hydroxyl groups in oxidized region**

2 We simulate the interlamination flow with 1000 water molecules between two kinds of GO sheets at  
3  $c=0.25$ . One is that the distribution of hydroxyl groups is sampled randomly in the oxidized region, and  
4 the other is sampled totally ordered as presented in Fig. 1. The water molecules were initially placed  
5 between two GO plates and we exerted the pressure of 0.5 atm on each plate to eliminate the void. A  
6 relaxation time was lasted for 500 ps in the NVT ensemble at 298 K. Afterwards, the exerting pressure on  
7 GO sheets was removed and we fixed the position of GO sheets. Finally, the  $d$ -spacing of the GO capillary  
8 is 1.64 nm, measured between two basal planes of GO laminates. The GO was treated as rigid during the  
9 whole simulation. The pressure-driven water flow by directly adding forces  $F = 0.042$  Kcal/mol to oxygen  
10 atoms in nonequilibrium molecular dynamics simulations. The simulation process lasted for a sufficiently  
11 long time (4 ns) at 298 K, and the sample evolved for 2.5 ns for data collection. The coordinates and  
12 velocities of all the atoms were recorded every 50 ps to get converged results.

13 We compared the flow characteristic of water between two kinds of oxidation distributions of GO  
14 surfaces by MD simulations. The spatial distributions of (a) density (b) potential energy (c) flow velocity  
15 along  $z$ -axis are portrayed in Fig. S2 (a)-(c). According to the spatial distribution of water density, we  
16 divided the laminated water into three parts: 1-layer from  $z = 6.25$  to  $9.25$  Å, 2-layer from  $z = 9.25$  to  $14.25$   
17 Å and 3-layer from  $14.25$  to  $17.25$  Å. The interaction energy between the water molecules in these three  
18 layers and GO surfaces have been recorded in Fig. S2 (d). It is observed that the flow characteristics is  
19 different when functional groups are totally ordered and random arrayed.

20

## 21 **2. Contact angle tests**

22 A series of contact angle tests have been performed on GO and graphene surfaces, and we compared  
23 the MD results with experiments in recent researches. The aim is to explain that the potential parameters  
24 in simulations can indicate the interaction between water molecules and hydroxyl groups.

25 MD simulations are generally limited to nanometer-sized water droplets, which leads to non-

1 negligible line tension force at the tri-phase junction. It results in the difference between the contact angle  
2 of a macroscopic water droplet and that of tiny size. Multiple simulations with water droplet of different  
3 sizes are required to deduce the contact angle of infinite droplet size, but this is computationally inefficient.  
4 We utilize a wetting system, which is free of size effect on the contact angle. A slab-like simulation box  
5 is adopted which is thin in  $y$ -direction and long in  $x$ -direction.<sup>1</sup> Periodic boundary conditions are applied  
6 to make the water droplet infinite in  $y$ -direction, like a truncated cylindrical cross-section. It is shown in  
7 Fig. S1. The advantage of this approach is that the contact line between water and substrate is straight,  
8 thus there is no contribution of line tension due to curvature. As a consequence, the macroscopic contact  
9 angle can be directly calculated through fitting the  $x$ - $z$  projection of the water droplet.

10 We simulate a series of samples with 4000 water molecules on copper (Cu), copper covered by  
11 graphene (CuG) and copper covered by GO (CuGO) surface. The water molecules in a well-defined order  
12 ~~was~~ were initially placed on substrates and then let them relax in the NVT ensemble at 298 K for a  
13 sufficiently long time ( $\sim 500$  ps), where the substrates were treated as rigid. Then the sample evolves for  
14 1 ns in the NVE ensemble for data collection. The snapshots and  $x$ - $z$  projection density distributions of the  
15 water droplets are shown in Figure S2 to S4. MD results shows that the contact angle (CA) equals to  
16  $83.33^\circ$  on Cu surface,  $87.69^\circ$  on CuG surface and  $45.35^\circ$  on CuGO surface. The coating film can control  
17 the wettability of a Cu surface. The graphene layers make substrates hydrophobic while the GO layers  
18 make them hydrophilic, which is agreement with previous researches.<sup>1-4</sup>

19

### 20 **3. Free energy analysis**

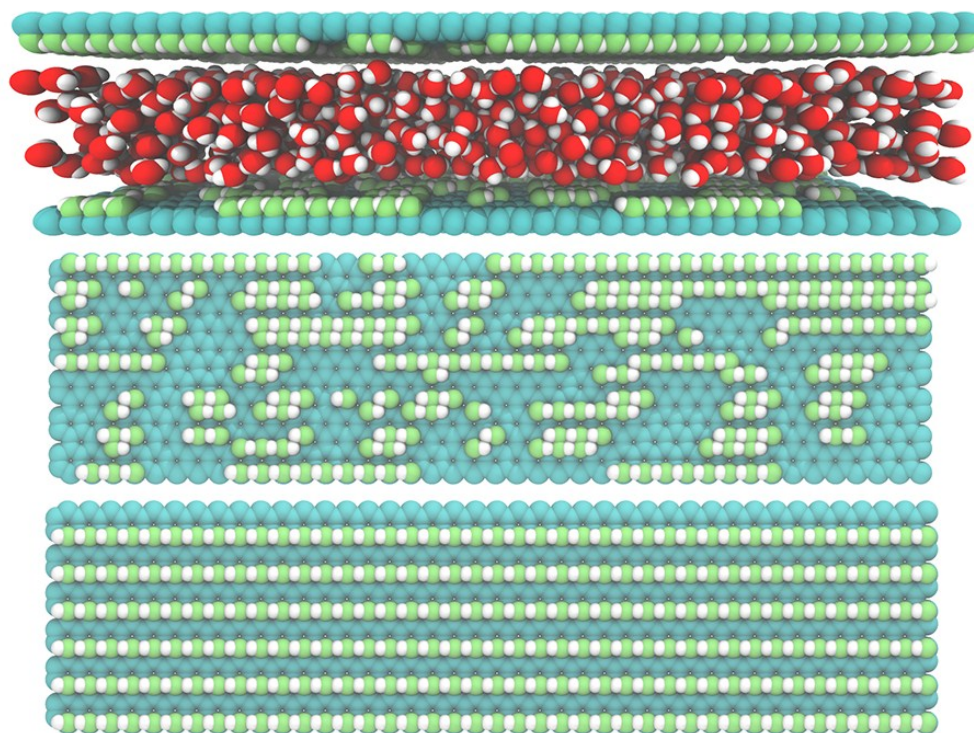
21 The free energy profiles are computed along the  $x$ -direction (i.e. perpendicular to the GO sheets), as  
22  $G(x) = -k_B T \ln(\rho(x))$ .<sup>5</sup> Figure S5 shows the free energy profiles of water between GO sheets with  
23 different concentrations ranged from 0.1 to 0.45. The extremely large energy barrier at  $x = 39 \text{ \AA}$  and  $x$   
24  $= 49.5 \text{ \AA}$  means the position of GO surface, where water molecules cannot arrive. With the increase of  
25 oxide concentration, the energy barrier near the wall surface escalate gradually. It indicates that water

1 molecules are impeded to move near the GO sheets for the existence of tremendous hydroxyl groups.

2

3

4



1

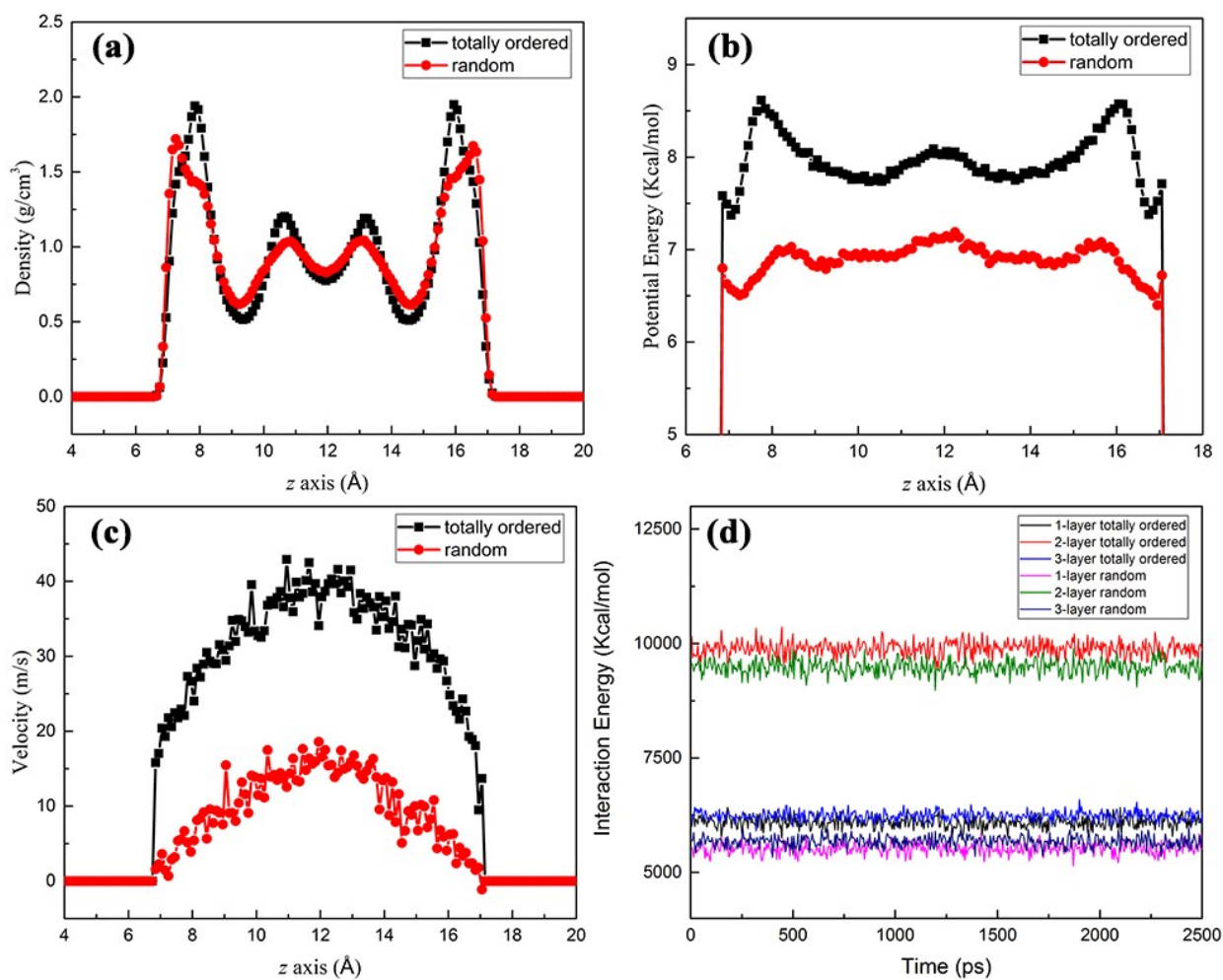
2 Figure S1. The initial configuration (top panel) of interlamination flow between two GO sheets at  $c=0.25$ .

3 The top view of GO sheet with functional groups randomly arrayed (middle panel) and totally ordered

4 (bottom panel). The dimensions are  $100.8 \text{ \AA} \times 25.6 \text{ \AA} \times 20 \text{ \AA}$ . Cyan, lime and white spheres are C, O and

5 H atoms of GO surfaces respectively. Red and white spheres denote O and H atoms in water molecules.

6



1

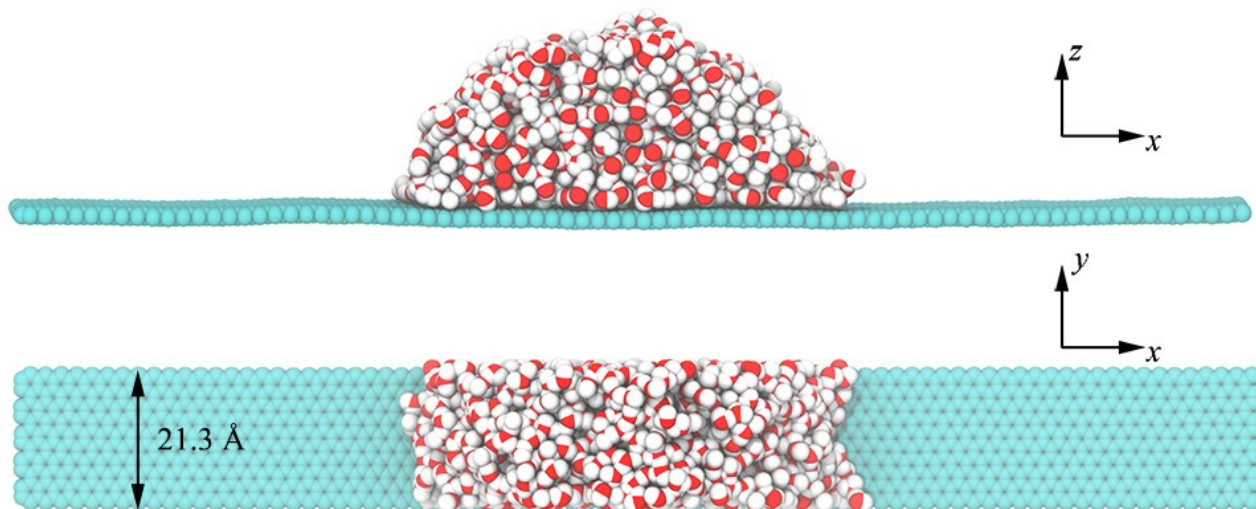
2 Figure S2. The flow characteristic of water between two kinds of oxidation distributions of GO surfaces.

3 (a) The spatial distribution of density along z-axis. (b) The spatial distribution of potential energy along z-

4 axis. (c) The spatial distribution of flow velocity z-axis. (d) The temporal evolution of interaction energy

5 between water molecules and GO surfaces.

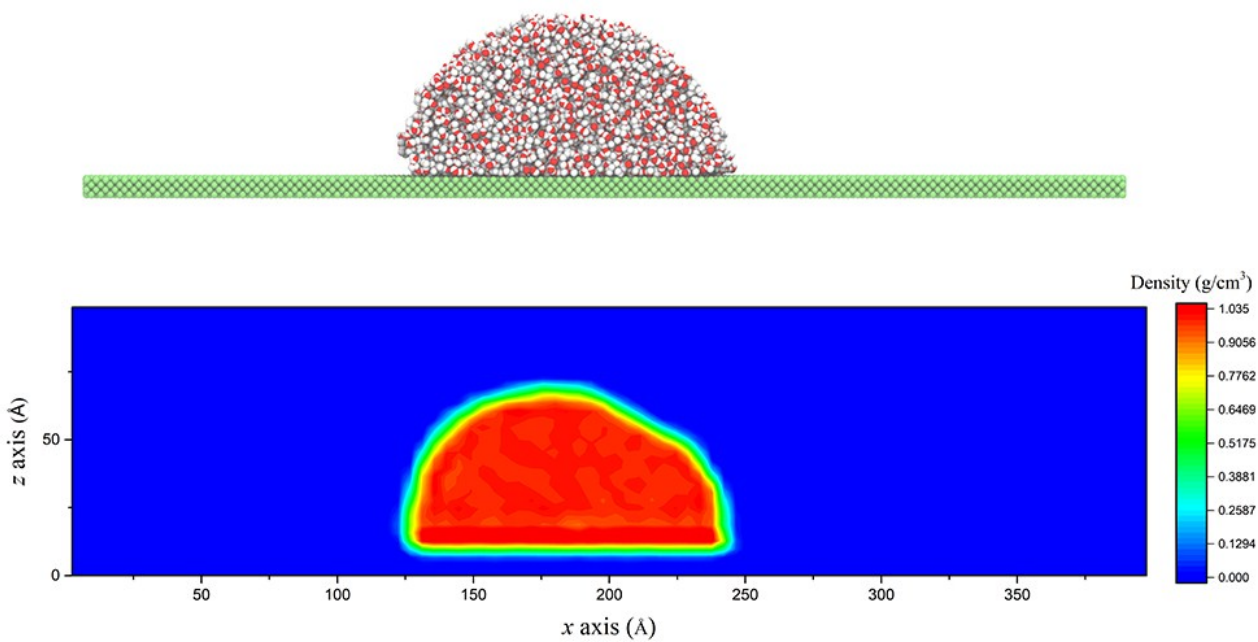
1



2

3 Figure S3. Side (top panel) and top view (bottom panel) of the snapshots for water droplet on graphene  
4 sheet. The dimensions are  $393.5 \text{ \AA} \times 21.3 \text{ \AA} \times 300 \text{ \AA}$ . Cyan, red and white spheres are C, O and H atoms  
5 respectively.

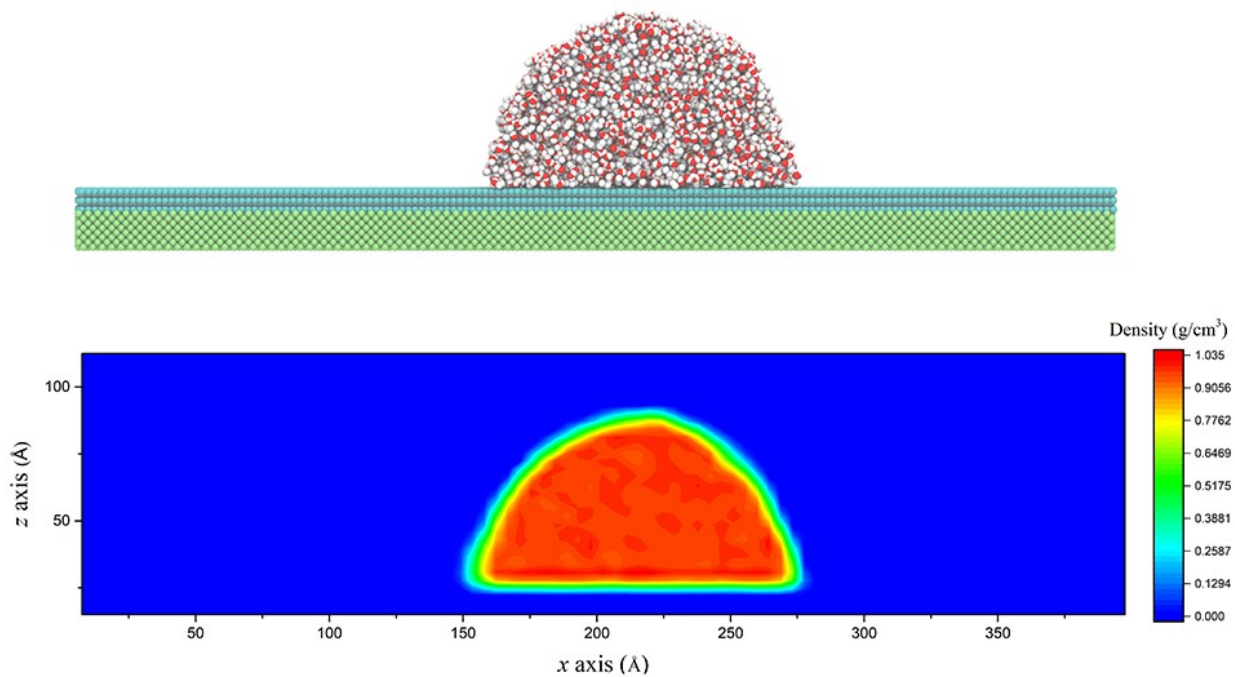
6



1  
2 Figure S4. The snapshot (top panel) and  $x$ - $z$  projection density distribution (bottom panel) of the water  
3 droplet on copper surface. Green, red and white spheres are Cu, O and H atoms respectively.

4

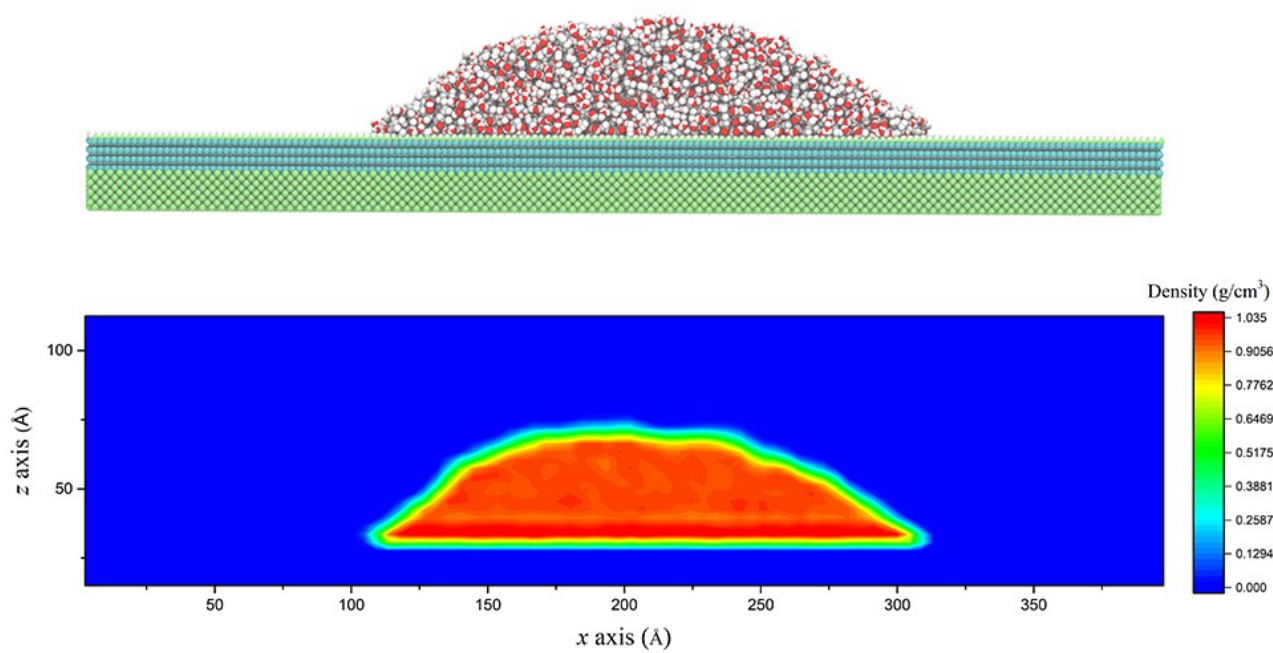
5



1

2 Figure S5. The snapshot (top panel) and  $x$ - $z$  projection density distribution (bottom panel) of the water  
3 droplet on copper covered by 3-layered graphene surface. Green, cyan, red and white spheres are Cu, C,  
4 O and H atoms respectively.

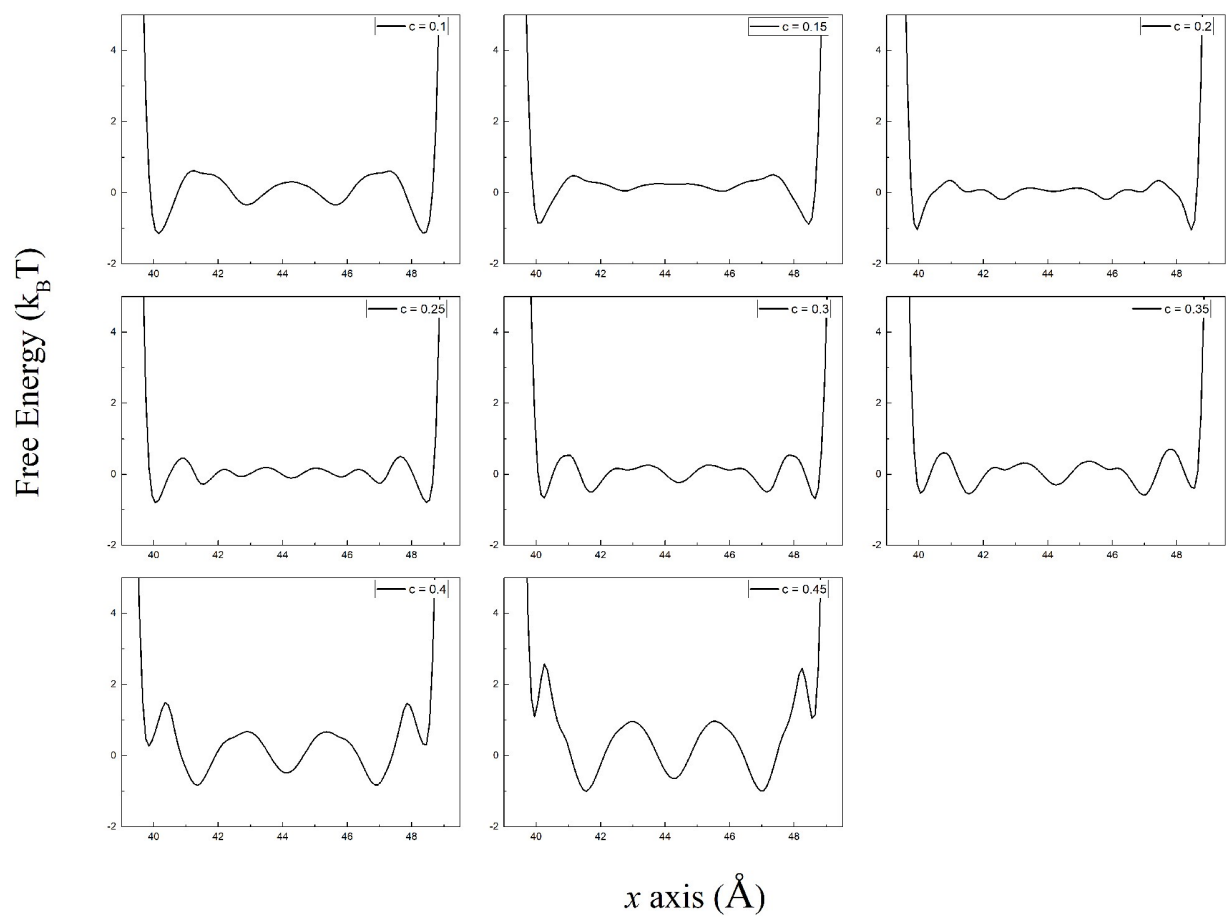
5



1

2 Figure S6. The snapshot (top panel) and  $x$ - $z$  projection density distribution (bottom panel) of the water  
3 droplet on copper covered by GO surface. Green, cyan, lime, white spheres are Cu, C, O and H atoms of  
4 surface respectively. Red and white spheres denote O and H atoms in water molecules.

5



1

2 Figure S7. Water free energy profiles between GO layers at different concentrations ranged from 0.1 to  
 3 0.45.

4

1 **4. References**

2

3 1. J. Rafiee, X. Mi, H. Gullapalli, A. V. Thomas, F. Yavari, Y. Shi, P. M. Ajayan and N. A. Koratkar,  
4 *Nat. Mater.*, 2012, **11**, 217.

5 2. J. Rafiee, M. A. Rafiee, Z. Z. Yu and N. Koratkar, *Adv. Mater.*, 2010, **22**, 2151.

6 3. Y. Dong, J. Li, L. Shi, X. Wang, Z. Guo and W. Liu, *Chem. Commun.*, 2014, **50**, 5586.

7 4. S. Zinadini, A. A. Zinatizadeh, M. Rahimi, V. Vatanpour and H. Zangeneh, *J. Membr. Sci.*, 2014,  
8 **453**, 292-301.

9 5. D. Cohen-Tanugi, L.-C. Lin and J. C. Grossman, *Nano Lett.*, 2016, **16**, 1027-1033.

10